

Multi-dimensional optical trapping of a mirror

Antonio Perreca,^{*} James Lough,[†] David Kelley,[‡] and Stefan W. Ballmer[§]

*Department of Physics, Syracuse University,
Syracuse, NY, 13244 - 1130, USA*

(Dated: March 19, 2014)

Alignment control in gravitational-wave detectors has consistently proven to be a difficult problem due to the stringent noise contamination requirement for the gravitational wave readout and the radiation-pressure induced angular instability in Fabry-Perot cavities (Sidles-Sigg instability). We present the analysis of a dual-carrier control scheme which uses radiation pressure to control a suspended mirror, trapping it in the longitudinal degree of freedom and one angular degree of freedom. We show that this scheme can control the Sidles-Sigg angular instability. Its limiting fundamental noise source is the quantum radiation pressure noise, providing an advantage compared to the conventional angular control schemes. In the appendix we also derive an exact expression for the optical spring constant used in the control scheme.

PACS numbers: 04.80.Nn, 07.60.Ly, 95.55.Ym

I. INTRODUCTION

The Laser Interferometer Gravitational-wave Observatory (LIGO) is part of a world-wide effort to detect gravitational waves and use them to study the universe [1]. Construction of LIGO's advanced detectors is underway. The installation is expected to finish in 2014. The goal of Advanced LIGO (aLIGO) is the first direct detection of gravitational-waves from astrophysical sources such as coalescing compact binaries and core-collapse supernovae. These detections will open a new spectrum for observing the universe and establish the field of gravitational-wave astronomy. These initial observations will also show the potential science gain of further increasing the state-of-the-art sensitivity of gravitational wave detectors [2–4]. Such detectors operate near the Standard Quantum Limit, meaning that the contributions from quantum radiation pressure and shot noise are about equal in the observation band [5, 6].

To design a successor to aLIGO, techniques to operate gravitational-wave interferometers below the Standard Quantum Limit need to be developed [7, 8]. Dual carrier control systems and angular control using stable optical springs are promising methods for evading quantum-mechanical limitations on detector sensitivity [9–14]. In 2007 Corbitt et al. at the LIGO Laboratory at the Massachusetts Institute of Technology demonstrated a one-dimensional optical trap of a one gram mirror using a novel two-carrier scheme [15]. Their work clearly demonstrated the potential of this technique. Extended to angular degrees of freedom, it has the prospect of opening a completely new approach to the angular control problem in future generation gravitational-wave detectors [16]. Sidles and Sigg have shown that, for a Fabry-

Perot cavity with a single resonating laser field, the radiation pressure force will couple the two end mirrors, always creating one soft (unstable) and one hard (stable) mode [17]. This sets a lower limit on the required angular control bandwidth, which inevitably results in higher noise contamination by angular control noise and limits the angular control performance in the first and second generation gravitational-wave interferometers [9, 18–20]. As we will show in section IV, angular optical trapping can bypass the Sidles and Sigg instability. Its fundamental noise limit is quantum radiation pressure noise, making it a promising candidate for low-noise angular control. Additionally, although we will not explore it in this paper, optical trapping of a mirror can be used to cool a mechanical degree of freedom. Depending on the mechanical system it can permit reaching the quantum ground state, enabling the manipulation of macroscopic object at the quantum level [21–25].

In this paper we present a prototype of a position and yaw optical trap for a suspended test mirror using a double dual-carrier control scheme. We propose a system with two longitudinal traps acting on different spots of a single mirror; together, these traps will constrain both the position degree of freedom and one angular degree of freedom of the mirror. This essentially replaces the current magnetic drives with optical traps. The idea is promising and will be easy to apply to the other angular degree of freedom. The model includes two optical cavities with the trapped end-mirror in common. Each cavity is illuminated with two overlapping laser beams at different frequency detunings - one is positive detuned (blue detuning) and the other is negative detuned (red detuning). The two dual-beams form two statically and dynamically stable optical springs with different lever arms and different power, designed such that the DC radiation pressure torques of the two dual beams cancel each other while DC radiation pressure force is canceled by displacing the position pendulum.

As a result, by picking the right parameters, we can obtain a system that is stable in the longitudinal and angular degrees of freedom with a mirror displacement

^{*}aperreca@syr.edu

[†]jdlough@syr.edu

[‡]dbkelley@syr.edu

[§]sballmer@syr.edu

range of the order of picometers.

The outline of this paper is as follows: In section II we review the idea of an optical spring. We then couple optical springs to a mechanical system and analyze the stability of the resulting opto-mechanical system. Section III extends the stability analysis to more than one dimension. In section IV we show that such a two dimensional optical spring is necessarily stronger than the Sidles-Sigg instability. In section V we calculate the radiation pressure noise, which is the fundamental limiting noise for radiation pressure control. Finally, in appendix A, we derive the approximation-free expression for the optical spring in a Fabry-Perot cavity, which to our knowledge has not been published yet.

II. STABILITY PRINCIPLE

An optically detuned Fabry-Perot cavity naturally leads to a linear coupling between intra-cavity power and mirror position. Depending on the sign of the detuning, this coupling creates an optical spring which is either statically stable or unstable. Due to the time delay in the optical field build-up, the optical spring restoration force is slightly delayed. This leads to a dynamically unstable spring for the statically stable case and a dynamically stable spring for the statically unstable case. Corbitt et. al. [15] demonstrated that by adding a second, frequency-shifted optical field (sub-carrier) with a different detuning and power, a statically and dynamically stable optical spring can be achieved. The dual-carrier scheme has been used to optically trap a gram-scale mirror, controlling its longitudinal degree of freedom. Moreover, the damping of the optical spring can be controlled by adjusting the detuning of both carrier and sub-carrier and their relative amplitudes. This naturally allows for efficient cooling of the degree of freedom seen by the optical spring. In contrast to a mechanical spring, this damping does not introduce intrinsic losses, and thus does not contribute to the thermal noise.

This technique can be extended to alignment degrees of freedom. By duplicating the Corbitt et al. approach for trapping with a second, different, optical axis and a different beam spot on the controlled mirror, it is possible to control the angular degree of freedom with radiation pressure alone.

To be able to understand the stability of multi-dimensional opto-mechanical systems, we first recall the simple driven damped mechanical oscillator. From there we will stepwise increase the complexity by adding optical springs and additional degrees of freedom.

A. Damped mechanical oscillator stability

Although the damped mechanical oscillator is a well known system, we will take it as a starting point to make

the reading clearer. Our goal is to describe the mechanical oscillator in the language of control theory, which allows us to understand the stability of the system from a different point of view. This approach can then be naturally extended to include the effect of additional optical springs.

The motion of a harmonic oscillator of mass m , spring constant k_m and velocity damping b , driven by the external force F_{ext} , can be expressed as [26]:

$$m\ddot{x} = -k_mx - b\dot{x} + F_{ext} \quad (1)$$

b is also called the viscosity coefficient. Often the damping rate $\Gamma = b/(2m)$ is used instead. Traditionally the equation of motion 1 is directly used to get the system's position response x when applying the external force F_{ext} . The resulting transfer function is

$$G = \frac{x}{F_{ext}} = \frac{1}{-m\Omega^2 + k_m + ib\Omega} \quad (2)$$

with Ω being the angular frequency of the motion.

Alternatively we can describe a damped mechanical oscillator as a feedback system, with the plant being just a free-test mass described by the transfer function $M = x/F_{ext} = -1/m\Omega^2$, obtained directly from the equation of motion of a free test-mass. The control filter of the feedback loop is the mechanical spring, which takes the mass displacement x as input and acts on the plant with the control signal, or force, F_K , which is subtracted from the external force F_{ext} . The transfer function of the control filter is $K_M = F_K/x = k_m + ib\Omega$. In this picture we can now calculate the closed loop transfer function and obtain the same expression as in equation 2:

$$G = \frac{M}{1 + K_MM} = \frac{1}{-m\Omega^2 + k_m + ib\Omega} \quad (3)$$

where $OL_M = -K_MM = (k_m + ib\Omega)/m\Omega^2$ describes the open loop transfer function of the system.

Stability

We can now check for the stability of the system in both pictures. We recall from literature that the stability of a system described by its transfer function G can be evaluated looking at the poles of its transfer function in the s -plane ($s = i\Omega$) [27]. In particular a system is stable only if its transfer function's poles have a negative real part, and the multiplicity of poles on imaginary axis is at most 1. The transfer function in equation 2 has the following poles:

$$i\Omega = -\frac{b}{2m} \pm \sqrt{\frac{b^2}{4m^2} - \omega_0^2}, \quad (4)$$

where $\omega_0^2 = k_m/m$ is the resonant frequency of the pendulum. The value of the damping rate $\Gamma = b/2m$

al. [15]. The carrier is set at a large positive detuning ($\delta > 0$, large δ/γ). This provides a static restoring force, together with a relatively small dynamic instability (anti-damping). Then a sub-carrier is added at lower power and with a small negative detuning ($\delta < 0$, small $|\delta|/\gamma$). The sub-carrier adds sufficient dissipation to stabilize the total optical spring, while leaving the sign of the static restoring force unchanged. For appropriately chosen parameters of carrier (c) and sub-carrier (sc) (power P_0^c and P_0^{sc} , detuning δ_c and δ_{sc}) the resulting total system thus becomes stable.

The spring constant of the total optical spring is simply the sum of the individual spring constants of the carrier and sub-carrier

$$K_{OS} = K_{OS}^c + K_{OS}^{sc} \quad (9)$$

where the individual springs K_{OS}^c and K_{OS}^{sc} are given by equation 8.

Conceptually we can think of the dual-carrier optical spring as a physical implementation of a feedback control filter for the mechanical system. With this tool at hand, we can start to analyze the behavior and stability of higher dimensional mechanical systems in the next section.

III. CONTROL MODEL OF LONGITUDINAL AND ANGULAR DEGREES OF FREEDOM

We will now extend our analysis to additional degrees of freedom. Experimentally, a torsion pendulum suspension is easy to build. Therefore we will focus our attention to controlling the yaw motion of a test mirror, keeping in mind that the method can be applied to any additional degree of freedom. For actively controlling two degrees of freedom (length and yaw), we need a two-dimensional control system. In other words, we will need a second dual-carrier optical spring in a setup that for example looks like Fig.2. We will label the two dual-carrier optical fields as beams A and B. Each beam includes a carrier and a sub-carrier field, i.e.

$$\text{Beam A} = \text{carrier A} + \text{sub-carrier A} \quad (10)$$

$$\text{Beam B} = \text{carrier B} + \text{sub-carrier B}$$

The two beams have a different optical axis, and each has its own optical spring constant, K_{OS}^A and K_{OS}^B , given by equation 9.

If we define x_A and x_B as the longitudinal displacement of the mirror at the contact points of beam A and beam B on the test mirror, and F_A and F_B as the corresponding exerted forces, we can describe the mechanical system with a plant matrix M :

$$\begin{pmatrix} x_A \\ x_B \end{pmatrix} = M \begin{pmatrix} F_A \\ F_B \end{pmatrix} \quad (11)$$

The explicit expression for M for a torsion pendulum is given in appendix B.

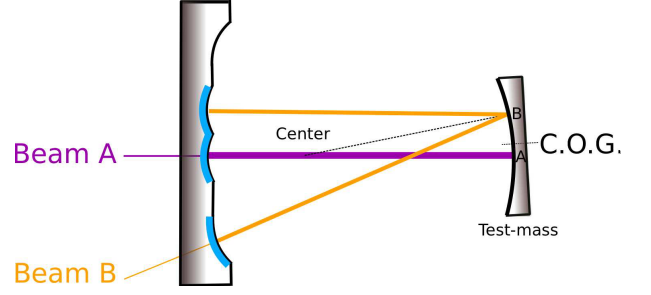


FIG. 2. In this sketch the main purple (Beam A) optical axis hits the test mirror at point A, slightly displaced from the center of gravity (C.O.G.), such that it still corresponds mainly to the length degree of freedom. Thus the second orange (Beam B) optical axis, which hits the test mirror closer to the edge at point B, needs much less power to balance the total DC torque. In our test setup the large input coupler is a composite mirror. It is 600 times more massive than the small mirror. The choice of a V-shaped beam B results in a more practical spot separation on the input coupler.

The control is provided by the optical springs. In the x_A - x_B basis the control matrix H is diagonal and given by (also see Fig.3)

$$\begin{pmatrix} F_A \\ F_B \end{pmatrix} = H \begin{pmatrix} x_A \\ x_B \end{pmatrix} = \begin{pmatrix} K_{OS}^A & 0 \\ 0 & K_{OS}^B \end{pmatrix} \begin{pmatrix} x_A \\ x_B \end{pmatrix} \quad (12)$$

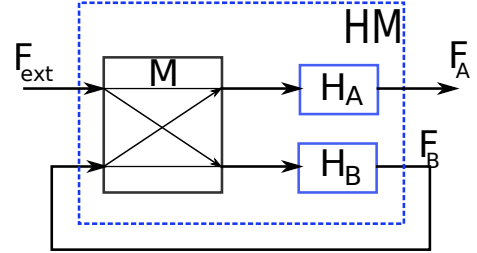


FIG. 3. Block diagram of beam A and beam B. The transfer function F_A/F_{ext} is equal to OL_A from equation 13. Each loop affects the other resulting in cross terms present in the matrix HM . M and $H_{A,B}$ are the transfer functions of the mechanical system and the optical springs of beam A and B, respectively.

For a multi-dimensional feedback system to be stable, it is sufficient that each individual (one-dimensional) feedback loop is stable, assuming all remaining control loops are closed. In other words, in our two-dimensional opto-mechanical system, we close the beam B control filter for evaluating the open loop transfer functions OL_A , and vice versa. For the open loop transfer functions OL_A and OL_B we then find:

$$OL_A = e_A^T (\mathbb{1} - HM(\mathbb{1} - e_A e_A^T))^{-1} H M e_A \quad (13)$$

$$OL_B = e_B^T (\mathbb{1} - HM(\mathbb{1} - e_B e_B^T))^{-1} H M e_B$$

with $e_A^T = (1, 0)$ and $e_B^T = (0, 1)$. The derivation of this expression is given in appendix C.

A. An Example

It is worth considering a specific set of possible values for our model and evaluate the control of angular and longitudinal degrees of freedom of a gram-scale test mirror using the radiation pressure of the light. All the optical fields involved in our analysis are derived from the same wavelength light source through frequency shifting. The model includes two optical cavities (Fig.2), referred to as beam A and B, both with an optical finesse of about 8000 and linewidth $\gamma/(2\pi) = 110$ kHz. The main cavity (beam A) is pumped with 1 W of carrier light, detuned by $\delta/(2\pi) = 250$ kHz (blue detuning, $\delta/\gamma = 2$), and 0.2 W of sub-carrier light, detuned by $\delta/(2\pi) = 60$ kHz (red detuning, $\delta/\gamma = -0.5$). This produces a statically and dynamically stable optical spring with a lever arm of 0.8 mm, measured from the payload center of gravity (C.O.G.). A second optical spring (beam B) is pumped with 6 times less power of carrier light, detuned by $\delta/(2\pi) = 186$ kHz (blue detuning, $\delta/\gamma = 1.5$), and 40 mW of sub-carrier light, detuned by 60 kHz (red detuning, $\delta/\gamma = -0.5$). This side cavity has a lever arm of 3.3 mm on the payload, such that the DC radiation pressure torques of beam A and B cancel. The DC radiation pressure force can be canceled by displacing the position pendulum.

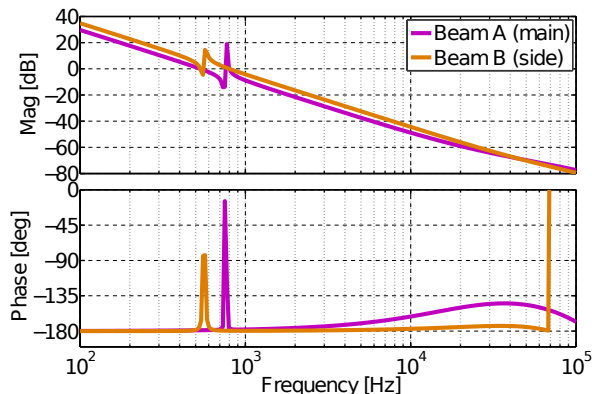


FIG. 4. Open loop gain (OLG) for the main and side cavity. The respective other loop is closed, and shows up as a resonance in the OLG. Note that, despite multiple unity gain crossings, both loops are stable because the resonances effectively implement a lead filter and the OLG avoids the critical point -1. Thus the dynamic interplay between multiple trapping beams on one payload does not introduce an instability.

The stability of the combined two-dimensional system is addressed in Fig.4. Plotted are the open loop gain functions of the two degrees of freedom (the two optical traps) under the assumption that the other loop is closed. The presence of the second loop introduces a resonance feature in each loop at the unity gain frequency of the other loop. However the open loop gain avoids the critical point -1 (phase at zero), leading to a stable system. The model parameters were intentionally tuned for low damping / high quality factor in order to demonstrate that the system remains stable. Lower quality factors,

and therefore stronger cooling is easily achievable.

B. Stability range

We can now estimate the robustness of our feedback control system by changing the microscopic length δx_A and δx_B of the two cavities. This changes the detuning of the optical springs for both beams. Therefore the propagators X_A and X_B for both beams change according to $X_{A,B} = r_1 r_2 e^{-i\delta_{A,B}\tau_{A,B}} \cdot e^{ik\delta x_{A,B}}$. For each position both the static and dynamical stability of the total optical spring system given by equation 13 is reevaluated.

In Fig. 5 the radiation pressure force due to the intra-cavity power of both beams versus the cavity offset is shown. The green shaded area represents the position range in which the two loops remain stable. The range is ~ 20 pm. The DC force fluctuations that the system can tolerate are given by the y-axis interval that the blue curve spends in the green shaded area.

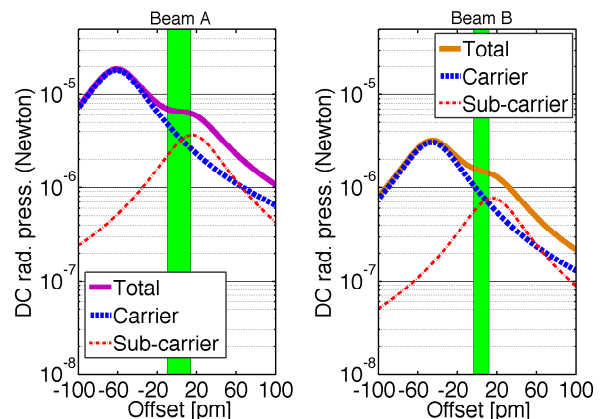


FIG. 5. Static carrier and sub-carrier build-up (calibrated in radiation pressure force) as a function of the respective cavity position. Also shown in blue is the total radiation pressure force. Using the stability testing method from section III B we find that the trap is both statically and dynamically stable in the green shaded area. With the chosen model parameters those regions are about 20 picometers wide.

IV. ANGULAR INSTABILITY

When operated with high intracavity laser power, suspended Fabry-Perot cavities like the arm cavities of LIGO have a well known angular instability. It arises from coupling the misalignment of the two cavity mirrors to radiation pressure torques. This is known as the Sidles-Sigg instability [17]. In this section we show that the intrinsic strength of an optical trap for alignment degrees of freedom is generally bigger, i.e. has a bigger spring constant than any associated Sidles-Sigg instability.

We start with a cavity of length L , with x_1, x_2 being the position of the beam spots on mirrors 1 and 2. θ_1, θ_2

are the yaw angles of the two mirrors, and R_1, R_2 are their radii of curvature. The corresponding g-factors are $g_{1,2} = 1 - L/R_{1,2}$. If one or both of the mirrors are slightly misaligned ($\theta_{1,2} \neq 0$), then the radiation pressure force exerts torques T_1 and T_2 on the two mirrors, given by the following relation (see for instance [17] or [30]):

$$\begin{pmatrix} T_1 \\ T_2 \end{pmatrix} = \frac{F_0 L}{1 - g_1 g_2} \begin{pmatrix} g_2 & -1 \\ -1 & g_1 \end{pmatrix} \begin{pmatrix} \theta_1 \\ \theta_2 \end{pmatrix} \quad (14)$$

with $F_0 = P_0 \frac{t_1^2}{(1-x)(1-\bar{x})} \frac{2r_2^2}{c}$ being the intra-cavity radiation pressure force. Sidles and Sigg first pointed out that, since the determinant of the matrix in this equation is negative, the two eigenvalues have opposite sign. This always leads to one stable and one unstable coupled alignment degree of freedom.

First we note that for a situation in which one mass is sufficiently heavy that we can neglect any radiation pressure effects on it (i.e. $\theta_1 = 0$), it is sufficient to choose a negative branch cavity (i.e. $g_1 < 0$ and $g_2 < 0$) to stabilize the setup. This is for instance the case for the example setup described in Fig. 2.

Next we want to compare the order of magnitude of this effect to the strength of an angular optical spring. If we call h the typical distance of the beam spot from the center of gravity of the mirror, and x the cavity length change at that spot, the order of magnitude of the optical spring torque is:

$$T \approx \frac{F_0 L}{1 - g_1 g_2} \cdot \frac{x}{h} \quad (15)$$

We can express this as the strength of an optical spring located at position h . The corresponding spring constant $K_{SS} \approx T/(hx)$. Thus we can see that

$$K_{SS} \approx \frac{F_0}{1 - g_1 g_2} \cdot \frac{L}{h^2}. \quad (16)$$

We now consider the adiabatic optical spring ($\Omega = 0$) in equation 7. Expressed in terms of F_0 , K_{OS} becomes

$$K_{OS} = iF_0 \frac{X - \bar{X}}{(1 - X)(1 - \bar{X})} 2k \quad (17)$$

Since we operate near the maximum of the optical spring, the order of magnitude of the resonance term can be estimated as

$$\frac{X - \bar{X}}{(1 - X)(1 - \bar{X})} \approx \frac{-i}{1 - |X|} \quad (18)$$

Thus we can estimate the magnitude of K_{OS} as

$$K_{OS} \approx F_0 \frac{4\pi}{\lambda} \frac{1}{1 - |X|} \approx F_0 \frac{4}{\lambda} \mathcal{F} \quad (19)$$

where \mathcal{F} is the cavity finesse. From equations 16 and 19 we see that the optical spring K_{OS} is much larger than the Sidles-Sigg instability spring K_{SS} if

$$h^2 \gg \frac{\lambda L}{\pi} \frac{1}{1 - g_1 g_2} \frac{\pi}{4\mathcal{F}} \quad (20)$$

Now recall that the beam spot size in a Fabry-Perot cavity is given by [31]

$$w_1^2 = \frac{\lambda L}{\pi} \sqrt{\frac{g_2}{g_1(1 - g_1 g_2)}} \quad (21)$$

Assuming a symmetric cavity ($g_1 = g_2$) for simplicity, we thus find that K_{OS} dominates over K_{SS} if

$$h^2 \gg w_{1,2}^2 \frac{1}{\sqrt{1 - g_1 g_2}} \frac{\pi}{4\mathcal{F}} \quad (22)$$

This condition is naturally fulfilled since we need to operate the angular optical spring with separate beams ($h > w_{1,2}$) and a large finesse ($\mathcal{F} \gg 1$). Therefore the angular optical spring is indeed strong enough to stabilize the Sidles-Sigg instability.

V. RADIATION PRESSURE NOISE

Another advantage of radiation pressure control, compared to a classical approach based on photo detection and feedback, is its fundamental noise limit. Unlike in the classical approach, the shot noise and other sensing noises never enter a radiation-pressure-based feedback loop. Even though technical laser noise is typically bigger in the simple cavity setup discussed in this paper, the only fundamental noise source of the scheme is quantum radiation pressure noise. In this section we give the full expression for radiation pressure noise in the case of a dual-carrier stable optical spring.

First, we note that as long as we are interested in frequencies much smaller than the any of the features in the detuned cavity transfer function, the radiation pressure noise is relatively simple. If we also assume that the end mirror has a reflectivity of 1, the one-sided ($f \geq 0$) radiation-force amplitude spectral noise density is given by

$$S_F(f) = \frac{2}{c} G \sqrt{2\hbar\omega P_{\text{in}}} \quad (23)$$

where G is the power gain of the cavity in the detuned configuration, and P_{in} is the power of the shot noise limited beam entering the cavity. Equation 23 is valid for carrier and subcarrier separately. Note that this equation does not hold if the end mirror has a finite transmissivity, as quantum fluctuations entering from that port will also contribute to the intra-cavity shot noise. In the case of a critically coupled cavity, this will result in an increase of the intra-cavity radiation-force amplitude spectral noise density by exactly a factor of 2.

To calculate the exact expression for the radiation pressure noise induced cavity fluctuations, we first realize that we can calculate the radiation-force amplitude spectral noise for a static cavity, and then compute the response of the dual-carrier optical spring system to that driving force. This yields the correct answer up to first order in the size of the quantum fluctuations. For the

calculation we track the quantum vacuum fluctuations entering at both ports of the cavity. It is useful to introduce a function F :

$$F(f) = F\left(\frac{\Omega + \delta + \omega_{res}}{2\pi}\right) = \frac{1}{1 - XY^2} \quad (24)$$

$$= \frac{1}{1 - r_1 r_2 e^{-2i\delta\tau} e^{-2i\Omega\tau}} \quad (25)$$

The amplitude build-up factors for fluctuations at frequency f entering through the input coupler (1) and the end mirror (2) thus are

$$t_1 F(f) \text{ and } r_1 t_2 F(f), \quad (26)$$

where we already dropped the one-way propagation factor because it drops out in the radiation force noise calculation below. We can now introduce the notation $F_0 = F(f_0)$, $F_+ = F(f_0 + f)$ and $F_- = F(f_0 - f)$. We then get the following expression for the one-sided radiation-force power spectral density for either carrier or sub-carrier.

$$S_F(f) = \frac{2}{c} S_P(f) \quad \text{and} \quad (27)$$

$$|S_P(f)|^2 = \hbar\omega P_0 t_1^2 |F_0|^2 (t_1^2 + r_1^2 t_2^2) (|F_+|^2 + |F_-|^2) \quad (28)$$

Here P_0 is the entering carrier power, and f_0 is its frequency. We can see that we recover equation 23 in the limit $t_2 \rightarrow 0$ and $G/t_1^2 = |F_0|^2 = |F_+|^2 = |F_-|^2$. The resulting force noise from carrier and sub-carrier for the cavity A in the example above is plotted in Fig.6 (top).

Next we calculate the response of the coupled opto-mechanical system to this driving force, using the following closed loop transfer function obtained from equations 11 and 12:

$$x = M(1 - HM)^{-1}F \quad (29)$$

Above the optical spring resonances this leads to a $1/f^2$ fall-off of the displacement noise, as expected for radiation pressure noise. Meanwhile below the resonance, due to the closed loop suppression, we will have a flat displacement noise. Fig.6 bottom illustrates this in the case of the two-dimensional angular trap discussed above.

Finally we compare the resulting displacement noise to a classical photo-detection feedback control scheme with similar control bandwidth and control loop shape. If such a system is able to detect all available power and has no other dominating sensing noise sources, it can at best achieve a shot noise sensitivity of

$$S_x \sim \frac{l}{P_0} \sqrt{2\hbar\omega P_0} \quad (30)$$

where l is the cavity line width in meters. To have the same control bandwidth and loop shape the system needs a controller transfer function equal to the optical spring, $H = K_{OS} \sim \frac{2GP_0}{cl}$, and hence it will have a noise performance similar to equation 23, $HS_x = S_F$. Thus we find that the traditional control scheme can only achieve similar noise if all the power from the cavity is detected, and there are no other relevant sensing noise sources.

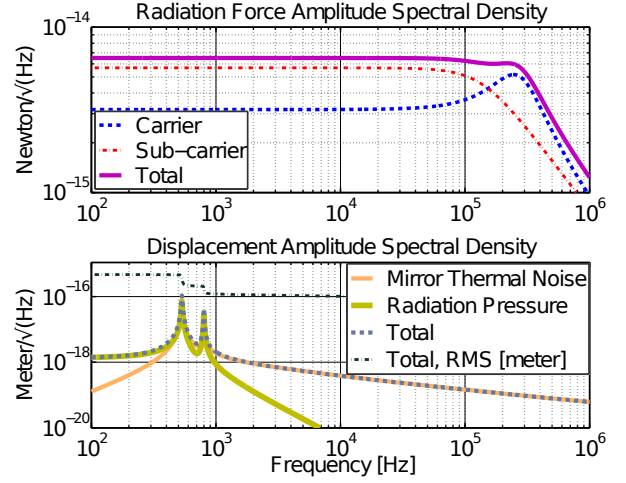


FIG. 6. (Top) Radiation force amplitude spectral density for the dual-carrier optical spring used in beam A of the above example. The sub-carrier dominates the noise at low frequency, but the higher-power carrier contributes more at high frequencies. Also note that if we choose the same free spectral range for the two carriers, there would be an additional beat note at the difference frequency of 310 kHz. (Bottom) Radiation pressure and thermal noise displacement amplitude spectral density. The radiation pressure noise is calculated using the opto-mechanical response given in equation 29. The thermal noise is based on a theoretical calculation described in [26], [30]. Since seismic and suspension thermal noise depend on the experimental implementation, they are not shown, but they would also be suppressed by the optical spring closed loop response. The residual RMS motion due to the shown noise sources is less than 10^{-3} picometer. With the total RMS motion smaller than the 20 picometer stability band shown in Fig.5, the two cavities will remain locked purely due to the radiation pressure trapping force.

VI. CONCLUSIONS

In conclusion, we investigated the use of the radiation pressure of the laser light as an alternative to a conventional feedback system for controlling the longitudinal and angular degree of freedom of a mirror. The method is based on a double dual-carrier scheme, using a total of four detuned laser fields in two cavities. The two dual-carrier beams hit the mirror in separate spots, forming two stable optical springs. This constrains both the longitudinal and the angular degrees of freedom of the mirror, replacing completely the commonly used electronic feedback system. We showed that this setup allows a stable control of the two degrees of freedom, within a displacement range of the test mirror of ~ 20 pm. This promising idea can be extended to the other angular degree of freedom. We found that such a method creates an angular optical spring stronger than the angular Sildes-Sigg instability, which drives the requirement for angular control in the high power arm cavities of gravitational wave detectors. We also showed that the fundamental limit

of this scheme is the quantum radiation pressure noise, resulting in a reduction in control noise compared to a conventional active feedback approach. We are working towards the experimental demonstration of this effect for a gram-scale mirror and beginning to explore its extension to large-scale gravitational wave detectors.

ACKNOWLEDGMENTS

We would like to thank Peter Saulson, Prayush Kumar, Riccardo Penco and Matt West for the many fruitful discussions. This work was supported by the National Science Foundation grant PHY-1068809. This document has been assigned the LIGO Laboratory document number LIGO-P1300224.

Appendix A: Optical spring constant derivation

In this section we consider the effect of light stored in a detuned Fabry-Perot cavity using a classical approach. The intra-cavity power generates radiation pressure that exerts on the cavity mirror a force $F_{rad} = -K_{OS} \cdot x$, where x is the mirror displacement and K_{OS} is the optical spring constant. Here we show the full derivation of the optical spring constant K_{OS} .

We consider a suspended Fabry-Perot cavity of length L_0 with an incident beam of wavelength λ and power P_0 . First we calculate a general expression of the intra-cavity power and then its radiation pressure force exerted on the end mirror.

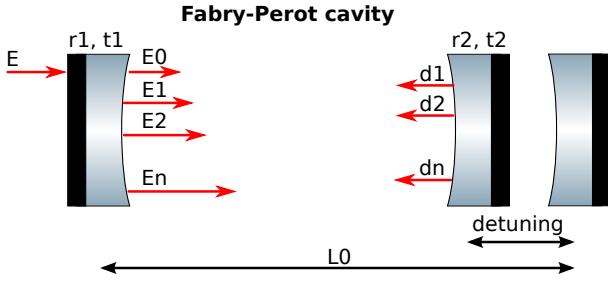


FIG. 7. A Fabry-Perot cavity of length L_0 and coefficients r_1, t_1 and r_2, t_2 for the input and end mirrors respectively. The input mirror is stationary while the end mirror is affected by harmonic motion. The incoming field E at each round-trip i adds up a phase shift due to the displacement d_i

The field $E = A_0 e^{i\omega t}$ enters the cavity through the input mirror of coefficient $t_1 = t$ and r_1 and the field inside the cavity at the input mirror can be seen as following

$$E_{tot} = E_0 + E_1 + E_2 + E_3 + \dots + E_n + \dots \quad (\text{A1})$$

We consider in our model the following definitions, with d_n being the displacement of the mirror,

$$\begin{aligned} L_1 &= 2(L_0 + d_1) \\ L_2 &= 2(2L_0 + d_1 + d_2) \\ L_3 &= 2(3L_0 + d_1 + d_2 + d_3) \\ &\dots \end{aligned} \quad (\text{A2})$$

with

$$\begin{aligned} d_n &= d(t - [(2n - 1)\tau + \alpha_n]) \quad \text{and} \\ \alpha_n &= 2 \sum_{l=1}^{n-1} \frac{d_l}{c} - \frac{d_n}{c} \end{aligned} \quad (\text{A3})$$

where $\tau = L_0/c$. With the round trip length $L = 2L_0$ we obtain

$$\begin{aligned} E_{tot} &= tE(1 + r_1 r_2 e^{-ikL_1} + (r_1 r_2)^2 e^{-ikL_2} \\ &\quad + (r_1 r_2)^3 e^{-ikL_3} \dots) \\ &= tE(1 + r_1 r_2 e^{-ikL} e^{-2ikd_1} + (r_1 r_2)^2 e^{-2ikL} e^{-2ik(d_1+d_2)} \\ &\quad + (r_1 r_2)^3 e^{-3ikL} e^{-2ik(d_1+d_2+d_3)} \dots) \end{aligned}$$

If we define $X = r_1 r_2 e^{-ikL}$ we have

$$\begin{aligned} E_{tot} &= tE(1 + X e^{-2ikd_1} + X^2 e^{-2ik(d_1+d_2)} \\ &\quad + X^3 e^{-2ik(d_1+d_2+d_3)} \dots) \end{aligned}$$

Since by definition the optical spring K_{OS} is the linear term in the expansion $F = F_0 + K_{OS}d + O(d^2)$, we now expand the exponential in d_n . We group d_n terms:

$$\begin{aligned} E_{tot} &= tE(1 + X(1 - 2ikd_1) + X^2(1 - 2ik(d_1 + d_2)) \\ &\quad + X^3(1 - 2ik(d_1 + d_2 + d_3)) + \dots) \\ &= tE(1 + X + X^2 + X^3 + \dots \\ &\quad - 2ikd_1(X + X^2 + X^3 \dots) \\ &\quad - 2ikd_2(X^2 + X^3 + X^4 \dots) \\ &\quad - 2ikd_3(X^3 + X^4 + X^5 \dots) + \dots) \\ &= \frac{tE}{1 - X}(1 - 2ikd_1X - 2ikd_2X^2 - 2ikd_3X^3 + \dots) \end{aligned}$$

Since any correction from α_n (equation A4) is quadratic in $d(t)$, we can again neglect it by definition, and find for the harmonic mirror motion (i.e. in the Fourier domain)

$$\begin{aligned} d_n &= x_0 e^{i\Omega t - (2n-1)\tau} = x_0 e^{i\Omega t} e^{-i\Omega(2n-1)\tau} \\ &= x_0 e^{i\Omega t} \frac{Y^{2n}}{Y} \frac{Y}{Y} = Y^{2n-2} d_1 \end{aligned} \quad (\text{A5})$$

where $Y = e^{-i\Omega\tau}$. Thus we can write

$$E_{tot} = \frac{tE}{1-X} (1 - 2ikd_1X - 2ikd_1Y^2X^2 - 2ikd_1Y^4X^3 - 2ikd_1Y^6X^4 \dots) \quad (A6)$$

$$= \frac{tE}{1-X} \times [1 - 2ikd_1X(1 + Y^2X + Y^4X^2 + Y^6X^3 \dots)] \\ = \frac{tE}{1-X} \left[1 - \frac{2ikd_1X}{1-Y^2X} \right] \quad (A7)$$

where d_1 is a complex number. Since we have to take its real part $Re(d_k) = \frac{d_k + \bar{d}_k}{2}$, we consider the field inside the cavity with \bar{d}_k conjugate of d_k :

$$\frac{tE}{1-X} \left[1 - \frac{2ik\bar{d}_1X}{1-\bar{Y}^2X} \right] \quad (A8)$$

and we obtain as total field E

$$E_{tot} = tE \left[\frac{1}{1-X} - \frac{2ikX}{2(1-X)} \left(\frac{d_1}{1-Y^2X} + \frac{\bar{d}_1}{1-\bar{Y}^2X} \right) \right]$$

and its complex conjugate

$$\bar{E}_{tot} = t\bar{E} \left[\frac{1}{1-\bar{X}} + \frac{2ik\bar{X}}{2(1-\bar{X})} \left(\frac{\bar{d}_1}{1-\bar{Y}^2\bar{X}} + \frac{d_1}{1-Y^2\bar{X}} \right) \right]$$

Using the following expression

$$d_1 = x_0 e^{i\Omega(t-\tau)} = x_0 e^{i\Omega t} e^{-i\Omega \tau} = xY \quad (A9)$$

we can now obtain the intra-cavity power expression by multiplying E_{tot} by its conjugate and considering only the linear terms of x

$$P = E_{tot} \cdot \bar{E}_{tot} = P_0 t^2 \left[\frac{1}{(1-X)(1-\bar{X})} - \frac{ikXxY}{(1-\bar{X})(1-X)(1-Y^2X)} - \frac{ikX\bar{x}\bar{Y}}{(1-\bar{X})(1-X)(1-\bar{Y}^2X)} + \frac{ik\bar{X}\bar{x}\bar{Y}}{(1-\bar{X})(1-X)(1-\bar{Y}^2\bar{X})} + \frac{ik\bar{X}xY}{(1-\bar{X})(1-X)(1-Y^2\bar{X})} \right] \quad (A10)$$

where we have also neglected the first constant term. We now group the terms in x and \bar{x} :

$$P = -P_0 t^2 \left[\frac{ikY}{(1-\bar{X})(1-X)} \left(\frac{X}{1-Y^2X} - \frac{\bar{X}}{1-Y^2\bar{X}} \right) x + \frac{ik\bar{Y}}{(1-\bar{X})(1-X)} \left(\frac{X}{1-\bar{Y}^2X} - \frac{\bar{X}}{1-\bar{Y}^2\bar{X}} \right) \bar{x} \right] = \\ = -P_0 t^2 \left[\frac{ikY}{(1-\bar{X})(1-X)} \times \left(\frac{X}{1-Y^2X} - \frac{\bar{X}}{1-Y^2\bar{X}} \right) x + cc \right] \quad (A11)$$

Once we have calculated the power we can obtain the radiation pressure force on the end mirror by $F_{rad} = \frac{2r_2^2}{c} P$. Furthermore we can also notice the similarity of the expression with the elastic force. Thus we recall that in frequency domain and complex notation K is defined by $F = -Kx$, the real form is thus

$$F' = Re[F] = -\frac{1}{2}(Kx + \bar{K}\bar{x}) = -\frac{1}{2}(Kx + cc)$$

Taking into account that we are calculating the radiation pressure on the end mirror, we need to consider an extra delay factor Y for the calculation of the power which appears in the expression of K . The complex spring is then given by

$$K = \frac{2r_2^2}{c} P_0 t^2 \frac{2ikY^2}{(1-\bar{X})(1-X)} \left(\frac{X}{1-Y^2X} - \frac{\bar{X}}{1-Y^2\bar{X}} \right)$$

which can be rewritten in the form of equations 6 and 7.

Detuning

Given the frequency detuning is $\delta = \omega_0 - \omega_{res}$ and $\Omega = \omega - \omega_0$, where ω_0 is the carrier (sub-carrier) frequency and ω_{res} is the resonant frequency, we get the following expressions:

Resonance

$$\lambda_{res} = L/n, \quad k_{res} = \frac{2\pi n}{L},$$

$$\omega_{res} = k_{res} \cdot c = \frac{2\pi n}{L} \cdot c \quad (A12)$$

Carrier

$$\lambda_0 = \lambda, \quad k_0 = \frac{2\pi}{\lambda} = k,$$

$$\omega_0 = k_0 \cdot c = \frac{2\pi c}{\lambda} = \omega_{res} + \delta \quad (A13)$$

Sideband

$$\omega = \Omega + \omega_0 = \Omega + \delta + \omega_{res} \quad (A14)$$

Thus we find

b. Matched cavity

$$\begin{aligned} e^{-ikL} &\equiv e^{-ik_0L} = e^{-i\omega_0 \frac{L}{c}} \\ &= e^{-i(\omega_{res} + \delta) \frac{L}{c}} = e^{-i\omega_{res} \frac{L}{c}} e^{-i\delta \frac{L}{c}} \end{aligned} \quad (\text{A15})$$

Recalling that $\tau = \frac{L_0}{c} = \frac{L}{2c}$ we can write

$$e^{-ikL} = e^{-i\delta 2\tau} \quad (\text{A16})$$

If we now replace X and Y we obtain the exact expression for K :

$$\begin{aligned} K_{OS} = & -P_0 t^2 r_2^2 \frac{4ike^{-2i\Omega\tau}}{c(1-r_1r_2e^{i2\delta\tau})(1-r_1r_2e^{-i2\delta\tau})} \times \\ & \left(\frac{r_1r_2e^{-i\delta\tau}}{1-r_1r_2e^{-2i\Omega\tau}e^{-i2\delta\tau}} - \frac{r_1r_2e^{i2\delta\tau}}{1-r_1r_2e^{-2i\Omega\tau}e^{i2\delta\tau}} \right) \end{aligned} \quad (\text{A17})$$

To compare to existing literature we now expand the exponentials to linear order in Ω and δ , $e^{-i\delta 2\tau} \approx 1 - i\delta 2\tau$ and $e^{-i2\Omega\tau} \approx 1 - i2\Omega\tau$:

$$\begin{aligned} K = & -P_0 t^2 r_2^2 \times \\ & \frac{4ik(1-2i\Omega\tau)r_1r_2}{c(1-r_1r_2+r_1r_2i2\delta\tau)(1-r_1r_2-r_1r_2i2\delta\tau)} \times \\ & \left[\frac{1-i2\delta\tau}{1-r_1r_2(1-2i\Omega\tau-i2\delta\tau)} - \frac{1+i2\delta\tau}{1-r_1r_2(1-2i\Omega\tau+i2\delta\tau)} \right] \end{aligned} \quad (\text{A18})$$

Considering the $Finesse \approx \pi \frac{r_1r_2}{1-r_1r_2} = \pi FSR/\gamma$, the cavity bandwidth γ , and the free spectral range $FSR = 1/2\tau$, we obtain:

$$\begin{aligned} K_{OS} \approx & -P_0 t^2 r_2^2 \frac{4ik(1-2i\Omega\tau)r_1r_2}{c(1+i\frac{\delta}{\gamma})(1-i\frac{\delta}{\gamma})(1-r_1r_2)^3} \\ & \times \left[\frac{1-i2\delta}{1+\frac{\Omega}{\gamma}i+\frac{\delta}{\gamma}i} - \frac{1+i2\delta}{1+\frac{\Omega}{\gamma}i-\frac{\delta}{\gamma}i} \right] \end{aligned} \quad (\text{A19})$$

Finally, since they correspond to a simple time delay, we neglect the $i\Omega\tau$, $i\delta\tau$ terms in the numerator and obtain

$$K_{OS} \approx P_0 t^2 r_2^2 \frac{8kr_1r_2}{c(1-r_1r_2)^3} \frac{\frac{\delta}{\gamma}}{(1+\frac{\delta^2}{\gamma^2})} \left[\frac{1}{1+\frac{\delta^2}{\gamma^2}-\frac{\Omega^2}{\gamma^2}+i2\frac{\Omega}{\gamma}} \right] \quad (\text{A20})$$

a. Overcoupled cavity

In the particular case of perfectly over-coupled cavity ($r_2 = 1$) $Finesse/\pi = 2/T_1$ and $(1-r_1r_2)^2 = T_1^2/2$ and the optical spring constant becomes:

$$K_{OS} \approx 128P_0 \frac{\pi}{c\lambda T_1^2} \frac{\frac{\delta}{\gamma}}{(1+\frac{\delta^2}{\gamma^2})} \left[\frac{1}{1+\frac{\delta^2}{\gamma^2}-\frac{\Omega^2}{\gamma^2}+i2\frac{\Omega}{\gamma}} \right] \quad (\text{A21})$$

In this case of a matched cavity ($r_1 = r_2$) $Finesse/\pi = 1/T_1$ and $(1-r_1r_2)^2 = T_1^2$ and the optical spring constant remains the same as in Eq. A21 except for the factor 128 which has to be replaced with 16.

Appendix B: Torsion pendulum mechanical plant

Here we transform the basis of coordinates $\{x_G, \Theta\}$ formed by the position of the center of gravity x_G of the mirror and its rotation angle Θ with respect to the vertical axis passing from x_G into a basis $\{x_A, x_B\}$ formed by the length of the cavities relative to beam A and beam B respectively. Thus the longitudinal and angular control of the mirror can be treated as the longitudinal control of the two above mentioned cavities. The basis can be expressed as

$$\begin{pmatrix} x_A \\ x_B \end{pmatrix} = \begin{pmatrix} 1 & r_A \\ 1 & r_B \end{pmatrix} \begin{pmatrix} x_G \\ \Theta \end{pmatrix} = \mathcal{B} \begin{pmatrix} x_G \\ \Theta \end{pmatrix} \quad (\text{B1})$$

with r_A and r_B being the lever arms of the two beams with respect to x_G .

The equation of motion for the mirror is

$$-\omega^2 \begin{pmatrix} m & \\ & I \end{pmatrix} \begin{pmatrix} x_G \\ \Theta \end{pmatrix} = \begin{pmatrix} F_{tot} \\ T_{tot} \end{pmatrix} \quad (\text{B2})$$

with I being the moment of inertia of the mirror of mass m . We now express the total force and the total torque exerted on the mirror as function of the individual forces F_A and F_B :

$$\begin{pmatrix} F_{tot} \\ T_{tot} \end{pmatrix} = \begin{pmatrix} 1 & 1 \\ r_A & r_B \end{pmatrix} \begin{pmatrix} F_A \\ F_B \end{pmatrix} = \mathcal{B}^T \begin{pmatrix} F_A \\ F_B \end{pmatrix} \quad (\text{B3})$$

Using equations B3 and B1 in equation B2 we obtain the equation of motion in the x_A, x_B basis:

$$-\omega^2 \left[\mathcal{B}^{T-1} \begin{pmatrix} m & \\ & I \end{pmatrix} \mathcal{B}^{-1} \right] \begin{pmatrix} x_A \\ x_B \end{pmatrix} = \begin{pmatrix} F_A \\ F_B \end{pmatrix} \quad (\text{B4})$$

Appendix C: Stability in two dimensions

The control loop stability in multiple dimensions can be evaluated by considering the one-dimensional open-loop transfer function of every control filter (i.e. optical spring) while all other loops stays closed. Here we calculate these open-loop transfer functions for the two-dimensional case.

Referring to figure 3, we inject a signal $F_{xa} = F_{ext}$ into port A. The output at port A is $F_{ya} = F_A$. We close the

loop from output B to input B by feeding back the force F_B . We obtain the following expression:

$$HM \begin{pmatrix} 0 \\ F_B \end{pmatrix} + HM \begin{pmatrix} F_{xa} \\ 0 \end{pmatrix} = \begin{pmatrix} F_{ya} \\ F_B \end{pmatrix} \quad (C1)$$

If we introduce the 2×2 matrix S :

$$S_A = \begin{pmatrix} 0 & 0 \\ 0 & 1 \end{pmatrix} \quad (C2)$$

we can write

$$HMS_A \begin{pmatrix} F_{ya} \\ F_B \end{pmatrix} + HM \begin{pmatrix} F_{xa} \\ 0 \end{pmatrix} = \begin{pmatrix} F_{ya} \\ F_B \end{pmatrix} \quad (C3)$$

Using the vector $e_A^T = (1, 0)$ we are able to extract the following open loop transfer function related to cavity A:

$$OL_A = \frac{F_{ya}}{F_{xa}} = e_A^T (\mathbb{I} - HMS_A)^{-1} HM e_A \quad (C4)$$

The same open loop transfer function can be obtained considering an external signal injected into the loop of the beam B while the loop of beam A remains closed.

$$OL_B = \frac{F_{yb}}{F_{xb}} = e_B^T (\mathbb{I} - HMS_B)^{-1} HM e_B \quad (C5)$$

with $e_B^T = (0, 1)$ and

$$S_B = \begin{pmatrix} 1 & 0 \\ 0 & 0 \end{pmatrix} \quad (C6)$$

-
- [1] B. P. Abbott, R. Abbott, R. Adhikari, P. Ajith, B. Allen, G. Allen, R. S. Amin, S. B. Anderson, W. G. Anderson, M. A. Arain, and et al., Reports on Progress in Physics **72**, 076901 (Jul. 2009), arXiv:0711.3041-[gr-qc].
 - [2] J. R. Smith and LIGO Scientific Collaboration, Classical and Quantum Gravity **26**, 114013 (Jun. 2009), arXiv:0902.0381-[gr-qc].
 - [3] G. M. Harry and LIGO Scientific Collaboration, Classical and Quantum Gravity **27**, 084006 (Apr. 2010).
 - [4] G. Losurdo, Classical and Quantum Gravity **29**, 124005 (2012), <http://stacks.iop.org/0264-9381/29/i=12/a=124005>.
 - [5] C. M. Caves, Physical Review Letters **45**, 75 (Jul. 1980).
 - [6] W.-T. Ni, Phys. Rev. A **33**, 2225 (Apr. 1986).
 - [7] S. L. Danilishin and F. Y. Khalili, Living Reviews in Relativity **15**, 5 (Apr. 2012), arXiv:1203.1706-[quant-ph].
 - [8] Y. Chen, Journal of Physics B Atomic Molecular Physics **46**, 104001 (May 2013), arXiv:1302.1924-[quant-ph].
 - [9] L. Document, LIGO-T1000416-v3 (30 Jul. 2010).
 - [10] V. B. Braginsky, S. E. Strigin, and S. P. Vyatchanin, Physics Letters A **305**, 111 (Dec. 2002), gr-qc/0209064.
 - [11] O. Arcizet, T. Briant, A. Heidmann, and M. Pinard, Phys. Rev. A **73**, 033819 (Mar. 2006), quant-ph/0602040.
 - [12] T. Corbitt, D. Ottaway, E. Innerhofer, J. Pelc, and N. Mavalvala, Phys. Rev. A **74**, 021802 (Aug. 2006), gr-qc/0511022.
 - [13] T. J. Kippenberg, H. Rokhsari, T. Carmon, A. Scherer, and K. J. Vahala, Physical Review Letters **95**, 033901 (Jul. 2005), physics/0506178.
 - [14] B. S. Sheard, M. B. Gray, C. M. Mow-Lowry, D. E. McClelland, and S. E. Whitcomb, Phys. Rev. A **69**, 051801 (May 2004).
 - [15] T. Corbitt, Y. Chen, E. Innerhofer, H. Müller-Ebhardt, D. Ottaway, H. Rehbein, D. Sigg, S. Whitcomb, C. Wipf, and N. Mavalvala, Phys. Rev. Lett. **98**, 150802 (Apr 2007).
 - [16] M. Punturo and et al., Classical and Quantum Gravity **27**, 084007 (Apr. 2010).
 - [17] J. Sidles and D. Sigg, Physics Letters A **354**, 167 (2006).
 - [18] V. Braginsky, S. Strigin, and S. Vyatchanin, Physics Letters A **287**, 331 (2001), ISSN 0375-9601.
 - [19] K. L. Dooley, L. Barsotti, R. X. Adhikari, M. Evans, T. T. Fricke, P. Fritschel, V. Frolov, K. Kawabe, and N. Smith-Lefebvre, J. Opt. Soc. Am. A **30**, 2618 (Dec 2013).
 - [20] E. Hirose, K. Kawabe, D. Sigg, R. Adhikari, and P. R. Saulson, Appl. Opt. **49**, 3474 (Jun 2010).
 - [21] J. D. Teufel, T. Donner, D. Li, J. W. Harlow, M. S. Allman, K. Cicak, A. J. Sirois, J. D. Whittaker, K. W. Lehnert, and R. W. Simmonds, Nature (London) **475**, 359 (Jul. 2011), arXiv:1103.2144-[quant-ph].
 - [22] A. D. O'Connell, M. Hofheinz, M. Ansmann, R. C. Bialczak, M. Lenander, E. Lucero, M. Neeley, D. Sank, H. Wang, M. Weides, J. Wenner, J. M. Martinis, and A. N. Cleland, Nature (London) **464**, 697 (Apr. 2010).
 - [23] J. Chan, T. P. M. Alegre, A. H. Safavi-Naeini, J. T. Hill, A. Krause, S. Gröblacher, M. Aspelmeyer, and O. Painter, Nature (London) **478**, 89 (Oct. 2011), arXiv:1106.3614-[quant-ph].
 - [24] T. Corbitt, C. Wipf, T. Bodiya, D. Ottaway, D. Sigg, N. Smith, S. Whitcomb, and N. Mavalvala, Phys. Rev. Lett. **99**, 160801 (Oct 2007).
 - [25] N. Matsumoto, Y. Michimura, G. Hayase, Y. Aso, and K. Tsubono, ArXiv e-prints (Dec. 2013), arXiv:1312.5031-[quant-ph].
 - [26] P. R. Saulson, Phys. Rev. D **42**, 2437 (Oct. 1990).
 - [27] A. L. Greensite, *Elements of modern control theory*, New York (Spartan Books, 1970).
 - [28] G. F. Franklin and A. Powell, J. D. Emami-Naeini, *Feedback Control of Dynamic System, USA, 3rd ed.* (Addison-Wesley Publishing Company, 1994).
 - [29] V. B. Braginsky and S. P. Vyatchanin, Physics Letters A **293**, 228 (Feb. 2002).
 - [30] S. W. Ballmer and D. J. Ottaway, Phys. Rev. D **88**, 062004 (Sep. 2013), arXiv:1306.0972-[gr-qc].
 - [31] A. E. Siegman, *Lasers* (University Science Books, 1986).